Eur Biophys J (1991) 19:189–201

European Biophysics Journal


# Measurements of transmembrane pH differences of low extents in bacterial chromatophores

## A study with the fluorescent probe 9-amino, 6-chloro, 2-methoxyacridine

**R. Casadio**

Section of Biophysics, Department of Biology, University of Bologna, I-40126 Bologna, Italy

Received March 19, 1990/Accepted in revised form September 5, 1990

**Abstract.** In chromatophores from photosynthetic bacteria the interaction of the fluorescent monoamine, 9-amino, 6-chloro, 2-methoxyacridine (ACMA), with the membrane is evaluated and described by an *S*-shaped adsorption isotherm. This phenomenon is hysteretic, as indicated by the difference between the adsorption and desorption branches of the binding isotherm. Maximal saturation of adsorption is reached at one ACMA per one to four lipid molecules, indicating that the probe binds in its neutral form. Adsorption of the probe on the membrane causes a large quenching of its fluorescence, which is explaind as being due to hypochromic effects following stacking and aggregation in a medium of low dielectric constant. A further quenching of fluorescence is brought about by imposing artificially induced transmembrane $\Delta$pH's. This latter phenomenon titrates in at increasing $\Delta$pH values and approaches saturation when $\Delta$pH is $\geqq 2$. The dependence of $\Delta$pH on the observed quenching of fluorescence is predicted by considering a model based on the equilibrium distribution of the amine between two phases at different pH's, in which adsorption of the probe on the membrane is used to evaluate its free concentration in the inner and outer compartments of the chromatophore vesicle. It is proposed that the equation thus obtained should be used to measure $\Delta$pH from the quenching of ACMA fluorescence.

**Key words:** Transmembrane pH difference – Fluorescent probes – Bacterial chromatophores – Adsorption isotherms

*Abbreviations:* $\Delta$pH, transmembrane pH difference between the inner and outer compartments; Q, quenching of fluorescence; BChl, Bacteriochlorophyll; ACMA, 9-amino-6-chloro-2-methoxyacridine; 9AA, 9-aminoacridine; Tricine, *N-tris*-(hydroxymethyl)methylglycine; MES, 2-morpholinoethanesulfonic acid; FCCP, carbonyl-cyanide-*p*-trifluoro-methoxy-phenylhydrazone; CCCP, carbonyl-cyanide-*m*-chloro-phenylhydrazone

## Introduction

Fluorescent amines are widely used to detect a transmembrane proton concentration difference ($\Delta pH_{i-o}$) in natural and model membrane systems in which direct measurements are generally precluded by the small dimensions of the inner osmotic volume (for review, see Rottenberg 1979; Baccarini Melandri et al. 1981; Azzone et al. 1985). According to the model first introduced by Schuldiner et al. (1972) amines are assumed to behave ideally, to be freely permeable through the membrane phase in their neutral form and to re-distribute between the inner and outer aqueous compartments following the protonation-deprotonation equilibria which occur upon the generation of a transmembrane $\Delta$pH (acidic inside). In the case of fluorescent amines, this equilibrium re-distribution is associated with a quenching of their fluorescence ($Q$) which, according to the model, would be promoted by accumulation of the probe in the inner aqueous compartment. This notion is based on the observation that the fluorescence is restored to its original level when the transmembrane $\Delta$pH is dissipated by effectors such as uncoupling agents, weak acids, ionophores and specific inhibitors of proton pumps. For monoamines of high $pK_a$ ($pK_a \gg pH_i$, $pH_o$) $\Delta$pH is therefore determined as:

$$\Delta pH_{i-o} = \mathrm{Log}\,(C_i/C_o) = \mathrm{Log}\,(Q/100-Q) + \mathrm{Log}\,(V_o/V_i)\,, \quad (1)$$

where $C_i$ and $C_o$ are the concentrations of the amine in the inner ($V_i$) and outer ($V_o$) aqueous compartments, respectively.

Over the past two decades, this model has been tested in our and other laboratories, mainly using the fluorescent monoamine, 9-aminoacridine (Deamer et al. 1972; Fiolet et al. 1974; Casadio and Melandri 1977, 1985; Haraux and de Kouchkovsky 1980; Hope and Matthews 1985; Vu Van et al. 1987). The conclusion of these experiments is that the probe behaves non-ideally, especially when it concentrates within the inner compartment of a vesicle system, and that this should be considered when applying Eq. (1).

Interactions of the acridinic dye with the membrane may be responsible for the observed deviation from the model of Eq. (1), particularly at low ionic strengths when screening of surface charges is reduced (Searle and Barber 1978). In negatively charged phosphatidylserine vesicles the quenching of 9-AA fluorescence could be due to $\Delta$pH-induced excimer formation of the excited molecules at the membrane, although other mechanisms cannot be excluded in natural systems or in lipid membranes of different composition (Grzesiek et al. 1989). An empirical calibration curve based on Eq. (1) can, however, correct for the non-ideal behaviour of the probe, as long as it is accepted that the quenching of fluorescence is associated with a $\Delta$pH formation, as the effect of $\Delta$pH effectors indicates. In chromatophores, the dependence of Log $(Q/100-Q)$ on the extent of artificially induced $\Delta$pH's is linear and has the predicted unitary slope (at least up to $2-2.5$ $\Delta$pH units). The estimates of the inner volumes which can be derived from Eq. (1) at $\Delta pH=0$, are, however, much higher than those obtained with independent direct measurements (up to thirty times when compared to the value of 15 µl per BChl micromol, as determined with EPR techniques by Melandri et al. (1984)]. It is therefore suggested that the value of the "apparent" inner volume, as calculated from the empirical calibration curves, is actually sufficient to account for the non-ideal behaviour of the probe when a $\Delta$pH value is evaluated from the corresponding quenching of fluorescence (Casadio and Melandri 1985). Interactions of 9AA with chloroplasts are evaluated in a similar way and included in Eq. (1), either by considering its partitioning between the membrane and the aqueous phases (Haraux and de Kouchkovsky 1980; de Kouchkovsky et al. 1984; Strotmann and Lohse 1988) or its specific binding at saturable binding sites on the membrane surface (Hope and Matthews 1985; Ve Van et al. 1987).

It is clear from Eq. (1) that the $V_o/V_i$ ratio sets a lower limit to the value of $\Delta$pH which can be evaluated from the quenching of fluorescent amines using the Schuldiner model. For example, the use of 9-aminoacridine is limited to $\Delta$pH's higher than $1-0.8$ units; this is because for membranes characterized by a phospholipid to protein weight ratio of about 1, the ratio of $V_o$ to the "apparent" $V_i$ is usually close to 1000 (Casadio et al. 1984). Assuming for simplicity that the value of the "apparent" $V_i$, as derived from calibration curves, is an approximate estimate of the tendency of any fluorescent probe to interact with the membrane domain, it can be seen from Eq. (1) that when this figure increases the same $\Delta$pH corresponds to increasing values of the quenching of fluorescence. This consideration, and the limitation of the use of 9-aminoacridine at high values of $\Delta$pH, prompted us to characterize (in the low $\Delta$pH region) the response of another fluorescent amine, 9-amino, 6-chloro, 2-methoxyacridine (ACMA), previously used to detect transmembrane proton flows in bioenergetics (Rydstrom 1979; Friedl et al. 1979; Malpartida and Serrano 1981; Dufour et al. 1982). ACMA seems to satisfy the above conditions since it is known that in photosynthetic membranes, in contrast to what is observed with 9-aminoacridine, the quenching of its fluorescence reaches saturation (90–100%) when the light-induced transmembrane $\Delta$pH is about $2-3$ units (Kraayenhof and Fiolet 1974; Fiolet et al. 1974). Indeed, in many studies aimed at characterizing proton pumping activities coupled to the ATP hydrolysis of ATPase complexes in natural and co-reconstituted systems the expected $\Delta$pH is low ($\leqq 1$). This is especially true in partially decoupled membranes or at the early stages of the $\Delta$pH onset (Casadio and Melandri 1984; Casadio 1988), and a suitable probe is required.

Being a 9-aminoacridine derivative, ACMA can exist as a dication protonated at the acridinic nitrogen and the amino group, a monocation protonated at the acridinic nitrogen, a neutral molecule, or an anion, when ionization of the amino group occurs. The spectral properties of these forms in solvents of different polarities and their corresponding acidity constants have been determined (Capomacchia and Schulman 1975; Marty and Viallet 1982, 1985; Marty et al. 1986). It is also known that this probe, unlike 9-aminoacridine (Gangola et al. 1981), does not dimerize in solution at concentrations as high as 200 µ*M* (Marty et al. 1986). In the range of physiological pH's, only the monocation-neutral molecule equilibrium is relevant ($pK_a=8.6$) and the monocation is the predominant form.

In this paper we characterize the optical properties of ACMA in the presence of un-energized and energized membranes, showing that the probe does not dimerize following accumulation at the solution-membrane interface or following $\Delta$pH formation and that the only fluorescent form of the probe is that free in the aqueous external compartment. Its time response in re-distributing across the membrane phase, at the onset of a transmembrane $\Delta$pH, is three times faster than that of 9-aminoacridine, probably due to its higher hydrophobicity.

Furthermore, from measurements of the partitioning of ACMA between the bulk phase and the membrane interface in the dark, we show that the interactions of the probe with the chromatophore system are mostly hydrophobic and can be described by a binding isotherm, in which adsorption occurs through a different modality than desorption.

It is then found that the experimental relation between artificially induced $\Delta$pH's and the corresponding quenching of fluorescence can still be predicted using the model based on the ideal behaviour of the amine provided that it is restricted to the aqueous compartments and that the two bulk concentrations of the probe are calculated by taking into account its binding to the membrane. This allows one to use the more realistic $V_i$ values measured with EPR techniques (Melandri et al. 1984) when the inner free concentration of the probe is calculated, at a given $\Delta$pH, from the binding isotherm and the overall mass balance. According to our data most of the dye is bound to the membrane even in the absence of a transmembrane proton concentration difference and using the model presented here, it is found that it remains adsorbed on the membrane interfaces in the presence of $\Delta$pH's as high as $2-3$ units. Thus the contribution of its free form in the inner compartment to the observed fluorescence is negligible. In conclusion, our results indicate that when ACMA is used to detect a transmembrane $\Delta$pH in chro-

matophores from photosynthetic bacteria, the dependence of $\Delta$pH on $Q$ is described by an S-shaped curve which must be used instead of Eq. (1).

## Materials and methods

### *Materials*

Inside-out vesicles (chromatophores) from photosynthetic bacteria were obtained by mechanical rupture of a photosynthetically grown green strain of *Rhodobacer capsulatus*, harvested at the end of the logarithmic phase of growth, as previously described (Baccarini Melandri and Melandri 1971). The protein and BChl contents of the preparations were analyzed by a modified Lowry procedure (Lowry et al. 1951) and as described by Clayton (1965), respectively. ACMA was purchased from Molecular Probes, Inc., Eugene, Oregon, USA.

### *Spectroscopic properties of ACMA*

Excitation and emission spectra of ACMA were recorded on a Jasco FP-550 or a Perkin Elmer MPF3 fluorimeter, equipped, when necessary, with polarizers. Absorbance spectra were measured using a Jasco Uvidec-610 double beam spectrophotometer. Calibration of the absorbance and emission intensities of ACMA in terms of concentrations was performed by measuring absorbance at 430 nm or fluorescence with excitation and emission wavelengths of 410 and 500 nm. This last wavelength pair was also used to monitor the quenching of fluorescence, which was routinely expressed as a percentage of the initial fluorescence intensity. Actinic light, produced by a 55-W quartz iodine lamp, was screened through an 88 A Wratten Kodak gelatin filter. ACMA was dissolved in ethanol at a final concentration of 2 m$M$, and as such was added to the assay media. When necessary, other solvents, such as cyclohexane, hexane, benzene, and 2,2,4-trimethylpentane were used. Corrections for inner filter effects and estimates of the relative quantum yields of the probe in solvents of different polarities were performed as described by Brandt and Witholt (1967).

The absorbance and emission intensities of ACMA in aqueous buffers were strictly proportional to the concentration in the ranges 2–150 and 0.1–50 $\mu M$, respectively. This was also verified when the ionic strength of the solution was changed from 0.1 to 0.25 $M$, by additions of Mg ions, or when the pH was changed from 6.5 to 8.5. An extinction coefficient of $5.1 \pm 0.2$ m$M^{-1}$ cm$^{-1}$ was determined for ACMA in the standard solution (see below). A 10–15% increase in the slope for the linear dependence of the fluorescence intensity upon the concentration of the probe was detected when Triton X-100 was present in the assay media (1–2% V : V). For each assay medium, a corresponding standard calibration curve for the fluorescence or absorbance intensities was used to determine the concentration of the probe.

Stopped flow fluorescence experiments were performed on a Biochem Sigma-Z W II spectrophotometer, equipped with a stopped flow apparatus and fluorescence attachment, as previously detailed (Casadio and Melandri 1985). The overall time resolution was less than 10 ms.

### *Measurements of the adsorption of ACMA at the solution-membrane interface*

Interactions of the probe with the membranes were measured by incubating in the dark, in a final volume of 8 ml, chromatophores corresponding to a BChl concentration of 20–40 $\mu M$, with known concentrations of the probe (routinely in the range of 1–50 $\mu M$). The standard assay medium was similar to that used to measure light-driven proton flows in chromatophores and contained 50 m$M$ Na-tricine, pH 8.5 (or 50m$M$ Na-MES, pH 6.5), 0.5 m$M$ $MgCl_2$ and 50 m$M$ KCl. Sodium succinate was also added at a concentration of 0.2 m$M$ to buffer the ambient redox potential. In control experiments it was shown that Mg ions at this concentration were necessary and sufficient to prevent adsorption of the probe (especially in the concentration range of 20–50 $\mu M$ and in the absence of the membrane phase) to the polycarbonate tubes (16 × 76.2 mm) utilized to spin down chromatophores. This was performed in a Type 65 fixed angle Beckman rotor, at 250 000 $g$ for 1 h at 25 °C. After this procedure a thick pellet was formed and the supernatants were collected and tested for their ACMA content using the appropriate calibration curves. Washing of the membranes was done by resuspending the pellets in the same standard assay medium, with increased concentrations of Mg ions when necessary, and re-pelletting the chromatophores. The volumes were rigorously adjusted to the initial value of 8 ml. Solubilization was achieved by incubating the pellets in 1 ml of the standard solution, containing 10% (V : V) of Triton X-100. After 6 h at 50 °C, or 24 h at 4 °C, the clarified suspensions were diluted (to a final volume of 8 ml) and the concentration of the probe was determined. Each experiment was done in triplicate and the average value of the concentration was considered. The experimental error was within 10%.

### *Calibration of the quenching of ACMA fluorescence in response to known $\Delta$pH's*

$\Delta$pH's were artificially imposed on chromatophore membranes using a procedure already described (Casadio and Melandri 1985), after equilibrating in the dark for 1 h at the initially imposed pH value. The quenching of ACMA fluorescence was recorded when pH transitions were induced, so that the pH was changed from acidic (routinely 5.5) to progressively increasing alkaline values, or from different initial values (ranging from 5.5 to 8.45) to a final alkaline value of 8.5. In either case, with the proton passive flow occurring in opposite directions, no significant difference of the $Q$ value for an imposed $\Delta$pH was detected. The initial and final pH of the suspensions were determined using a Radiometer PH M 62 pH meter, and the $\Delta$pH was calculated. The concentration of sucrose, when

present, was 1.25 *M*. Photophosphorylation and ATPase activity in the dark, which depend on the ACMA-BChl molar ratio, were measured as previously described (Baccarini Melandri and Melandri 1971).

*Theoretical evaluation of ΔpH from the quenching of ACMA fluorescence*

The data were analyzed with an Olivetti M 240 personal computer, equipped with a Tektronix 4662 interactive digital plotter. Curve fitting was performed using a non-linear least squares minimization routine based on a gradient-expansion algorithm, as described by Bevington (1969). Free ACMA concentrations were calculated from the adsorption isotherm by means of an iterative procedure used to compute the ΔpH corresponding to a given quenching of fluorescence. During the search loop, the condition of convergence between the right and the left side of the equation was set within 0.01%. To be more specific, the iterative procedure comprises the following steps: *1)* The value of the free bulk concentration of ACMA corresponding to a certain amount of probe added to the chromatophore suspension is experimentally known. The overall amount of the ACMA, $n^T$, is then re-evaluated from Eq. (3), after calculating the corresponding surface concentration, $\sigma S$, as the numerical solution of Eq. (4) by means of the root-finding routine of Newton-Raphson (William 1986); *2)* The external free concentration of the probe, in the presence of the ΔpH, is then calculated as a function of the $Q$ value [Eq. (6)] and its corresponding surface density is again the numerical solution to Eq. (4). The adsorbing parameters depending on the adsorbing area (namely $\sigma_{max} S$ and $A$) are expressed in terms of the external surface area by considering the ratio between the external and total adsorbing membrane surface; *3)* From the above, and from the mass balance of Eq. (2), the amount of ACMA in the inner bulk and membrane face ($n_i$) is calculated. The relation $n_i = C_i V_i + \sigma_i S_i$ is used, in combination with Eq. (4) (in which the parameters of the desorption isotherm are modified so as to include the fraction of total adsorbing surface corresponding to the internal one) and $C_i$ is determined by knowing $V_i$; *4)* ΔpH is calculated, after evaluating the internal pH with Eq. (5). By this procedure, the ratio of the external and inner surfaces to the total adsorbing area of the membrane is determined when the calculated ΔpH for a given $Q$ corresponds to the experimental one.

## Results

*Spectroscopic properties of ACMA in the presence of chromatophore membranes*

At pH 8.5, which is that required for maximal ATPase activity in chromatophore membranes (Casadio and Melandri 1984), the excitation spectrum of ACMA in an aqueous buffered solution with an ionic strength of 0.1 *M* is characterized by one maximum at 412 nm and two shoulders centered at 384 and 429 nm. This corresponds to the pattern observed in the absorption spectrum under the same experimental conditions (not shown). The fluorescence emission spectrum is, in turn, characterized by a broad band centered at 478 nm. The absorbance of ACMA is proportional to its concentration in the range 0.1–150 μ*M* (measured as described in the Material and methods section). The excitation and emission intensities are also found to be proportional to the concentration from 0.1 to 50 μ*M*, so that calibration curves of fluorescence intensities as a function of concentration may be constructed and used to determine the probe concentration when necessary. These optical parameters are unaffected by changing the ionic strength of the medium from 0.01 to 0.25 *M* or the pH from 6.5 to 8.5.

When chromatophores are added to the assay medium at an ionic strength of 0.1 *M* the following changes of the spectroscopic properties are detected. The absorption (not shown) and fluorescence excitation spectra (Fig. 1 A), although unaffected with respect to their shapes and positions of the maxima, are characterized by a diminished intensity in the wavelength range studied. This decrease titrates in at increasing concentrations of BChl (1–40 μ*M*). The fluorescence emission spectrum shows a large reduction in intensity and a change in band shape (Fig. 1 B). The broad band characteristic of the emission spectrum of ACMA in solution splits into two bands of different intensities, centered at 470 nm (the less intense) and at 508 nm (the more intense). This splitting, in parallel with the progressive decrease of the intensity, is again brought about by increasing the concentration of chromatophores, with respect to the concentration of ACMA. When corrections for inner filter effects are done, the original shape of the emission spectrum can be restored, whereas the decrease of the fluorescence intensity with respect to that of ACMA in solution is maintained (Fig. 1 B). This indicates that the splitting observed in the emission spectrum is caused by overlapping of the ACMA emission with the absorption spectrum of the carotenoid pigments present in the chromatophore membranes and absorbing in the 400–500 nm region (this absorption spectrum is characterized by three maxima, centered at 430, 475 and 489 nm, respectively). The observed decrease of intensity can be explained by assuming that in the presence of chromatophores the absorption and excitation spectra of the probe, when embedded within the hydrophobic membrane domain, are blue-shifted following adsorption. They would then become undetectable due to overlapping with membrane pigments in the visible region or with protein chromophores if it is considered that the shift may also include the near ultraviolet region. Under these conditions, its fluorescence is also severely quenched in the wavelength range studied. This is consistent with the observation that when ACMA is dissolved in apolar solvents its excitation and emission spectra are progressively blue-shifted (e.g., in cyclohexane the excitation maximum is at 370 nm) on decreasing the polarity of the solvent (according to the polarity scale of Kamlet et al. 1977). Concomitantly, the relative quantum yield of fluorescence is highly decreased by up to ten times (our unpublished observations; Marty and Viallet 1982).

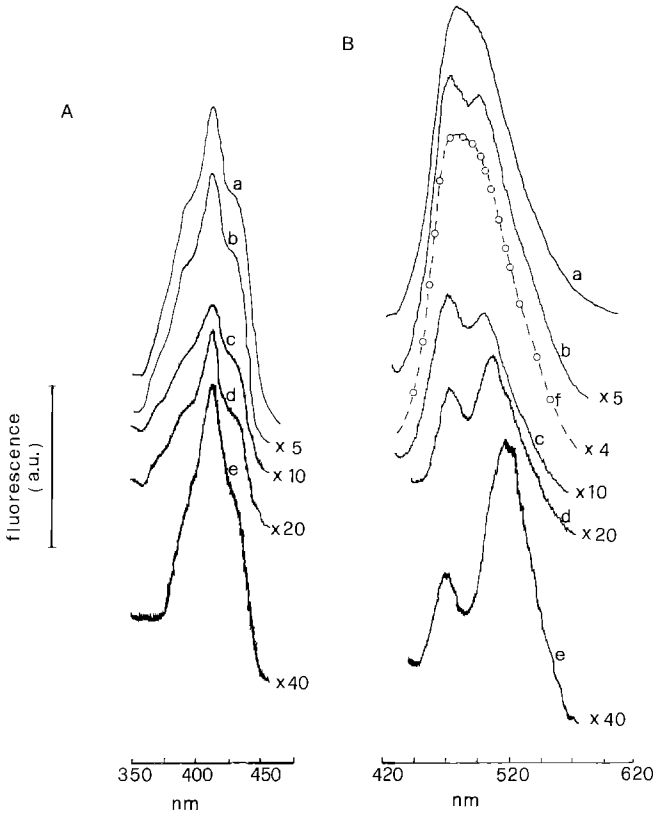


**Fig. 1 A, B.** Excitation and emission spectra of ACMA in the presence of chromatophores from photosynthetic bacteria. Excitation (**A**) and emission (**B**) spectra were recorded by setting the emission and excitation wavelengths at 500 and 410 nm, respectively. **A** excitation spectrum of 5 $\mu M$ ACMA in the absence of chromatophores (in aqueous buffer at pH 8.5, $I = 0.1\,M$); (b) to (e): as (a) but with addition of chromatophores corresponding to 2, 5, 10, and 20 $\mu M$ BChl, respectively. **B** (a) to (e): as in Fig. 1 A; (f): spectrum (e) after correction for inner filter effects

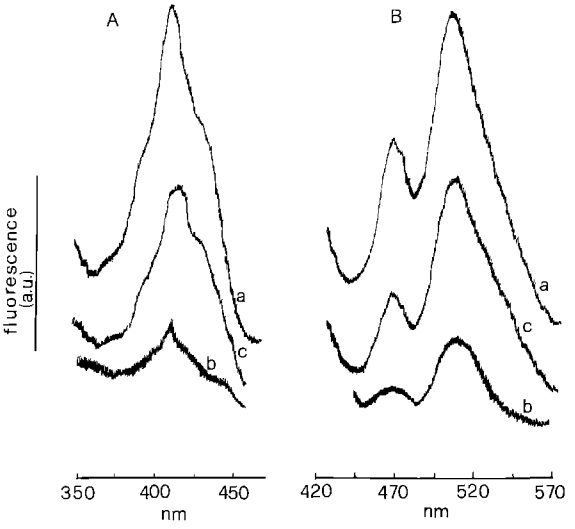


**Fig. 2 A, B.** Excitation (**A**) and emission (**B**) spectra of ACMA in the presence of chromatophores during energization with actinic light. **A** (a): excitation spectrum of 5 $\mu M$ ACMA in the presence of chromatophores corresponding to 30 $\mu M$ BChl; (b): as (a), under energization with actinic light; (c): as (b) in the presence of 0.05 $\mu M$ nigericin. **B** conditions as in Fig. 2 A. Excitation and emission spectra of ACMA recorded after energization, or under energization in the presence of nigericin 2 $\mu M$, are coincident with spectra (a) in **A** and **B**, respectively

We conclude that the only excited and emitting species of the probe in the presence of the membrane system is that free in the aqueous environment. Consistently, upon addition of chromatophores, the spectral shape of the emission is unaffected when parallel or crossed polarized fluorescence is detected (not shown).

After incubation of the amine with chromatophores in the dark the distribution of ACMA between the membrane and the bulk aqueous phases reaches equilibrium, as indicated by the fact that the observed fluorescence reaches a steady-state level. A further quenching of the fluorescence of the probe can be observed either by illuminating chromatophores with a red actinic light or by imposing artificial $\Delta$pH's across the membrane with acid to basic transitions (see below). In the first case, when the transmembrane $\Delta$pH is maintained at stationary state by the photosynthetic activity the quenching of fluorescence is as high as 100%. This figure can be diminished upon addition to the assay medium of limited amounts of nigericin, or other effectors of the transmembrane $\Delta$pH in biological membranes. The excitation and emission spectra of ACMA were recorded in the light and the quenching of fluorescence was found to be 60% in the presence of nigericin (0.05 $\mu M$) and 98% in its absence (Fig. 2 A, B). In both cases the spectra kept the same shape and peak positions but the intensity was decreased over the full wavelength range.

This suggests again that the quenching of fluorescence observed is due to a further association of the probe with the membrane phase and that, when the probe is entering this phase, it is no longer contributing to the emission spectra. In the presence of energized membranes, as with experiments in the dark, it was not possible to detect splitting of the maxima in the excitation spectrum. The splitting would be associated with dimer or multimer formation (Albert 1966; Torres Pereira et al. 1984).

It can therefore be concluded that under these experimental conditions there is no evidence for dimer formation upon further association of the probe with the membrane and that the only fluorescence detected is that due to the probe free in the aqueous environment.

The initial level of fluorescence is restored, over the whole wavelength interval, by switching off the actinic light (the time interval for full recovery was less than 1 s in the presence of valinomycin), or by adding, in the light, nigericin, FCCP or CCCP at micromolar concentrations.

### *Characterization of the partitioning of ACMA between the aqueous phase and the membrane interface*

Adsorption of the probe on the membrane was determined after equilibrating aqueous suspensions containing chromatophore membranes and ACMA (added as ethanolic solutions) at final concentrations ranging from 1 to 50 $\mu M$. These experiments were performed in the dark, to avoid formation of a transmembrane $\Delta$pH, and

in the presence of valinomycin and potassium ions, so that, under these experimental conditions, the transmembrane potential difference is also negligible (Casadio and Melandri 1984). After centrifugation of the suspensions, the concentrations of ACMA free in the bulk solutions were determined from the fluorescence and absorbance intensities of the aqueous supernatants, using calibration curves previously obtained in the same buffer solution. The procedure is detailed in the Materials and methods section.

An example of the results obtained on incubating chromatophores corresponding to a fixed concentration of BChl with variable amounts of the probe is given in Table 1. The amount of ACMA recovered in the supernatants (second row of Table 1) after pelletting the chromatophore membranes is about 20–30% of the quantity initially added to the samples. The remaining ACMA is bound to the membrane (third and fourth rows in Table 1). Resuspension and washing of the pellet causes a release into the aqueous solutions of some 10–15% of the total amount of ACMA found within the membrane domain. These data are unaffected, within experimental error, when $Mg^{2+}$ is added to the buffer at concentrations as high as 50 m*M*. The remaining 85–90% is recovered only upon subsequent solubilization of the membrane or by extensive washing of the pellets, which causes release of ACMA into the aqueous solutions (data not shown).

During these experiments the pH is rigorously maintained at 8.5, when 44% of the probe concentration is present in a neutral form ($pK_a = 8.6$). It is worth mentioning, however, that within experimental error, the results obtained are not affected by lowering the pH to 6.5 (and almost doubling, therefore, the percentage concentration of the monocation as compared to pH 8.5), while keeping the ionic strength constant.

On the basis of these results one can exclude the possibility that adsorption of the probe on the membrane is dependent on the concentration of the amine monocation at the solution-membrane interface or on the ionic strength of the bulk solution in the range from 0.1 to 0.25 *M*.

**Table 1.** Partitioning of ACMA between the aqueous phase and the membrane interface

| $ACMA_T$ (nmoles) | $ACMA_S$ (nmoles) | $ACMA_{S1}$ (nmoles) | $ACMA_P$ (nmoles) | $ACMA_R$ (%) |
|---|---|---|---|---|
| 12.8 | 2.9 | 0.3 | 5.6 | 69 |
| 24.4 | 5.2 | 0.5 | 12.7 | 75 |
| 32.1 | 10.2 | 2.0 | 20.5 | 100 |
| 64.0 | 14.2 | 3.9 | 33.9 | 81 |
| 128.5 | 22.9 | 8.6 | 73.6 | 82 |
| 256.0 | 31.8 | 26.2 | 182.4 | 94 |
| 384.0 | 60.5 | 41.6 | 219.2 | 84 |

The experimental conditions are detailed in the Materials and methods section. Each experiment was performed in triplicate and the experimental error is within 10%. $ACMA_T$: nanomoles of ACMA added as ethanolic solution to a final volume of 8 ml containing chromatophores corresponding to 20 μ*M* BChl. $ACMA_S$: nanomoles of probe free in the aqueous supernatant after pelletting the membranes. $ACMA_{S1}$: the membranes have been re-suspended and re-pelletted. $ACMA_P$: after solubilization of the pellet, obtained upon the second washing, with Triton X-100. $ACMA_R$: recovery of the total mass of the probe added to the assay

The distribution of the probe between the membrane and the aqueous phase can be described, for simplicity, by a three step model in which the permeation of the molecule through the membrane phase comprises adsorption at the external water-membrane interface, diffusion to the opposite internal face and desorption into the osmotic internal phase. Therefore, when the mass balance for the total number of ACMA molecules ($n^T_{(ACMA)}$) is considered, the following equation is derived:

$$n^T_{(ACMA)} = (C_o V_o + \sigma_o S_o) + (C_i V_i + \sigma_i S_i) . \quad (2)$$

According to this hypothesis the free concentration of the molecule in the outer ($C_o$) and the inner ($C_i$) phase is at equilibrium with and is dependent on its corresponding surface density ($\sigma_o$ and $\sigma_i$, respectively) as predicted by an appropriate adsorption isotherm. In this model no distinction is made between the neutral and the monocation forms of the probe. As our results indicate, either both forms of the amine bind to a region which is not accessible to the solution (so that this hypothetical binding face is located in the boundary region below the water-membrane interface), or only the neutral species of the amine adsorbs on the solution-membrane interface and the protonation-deprotonation equilibria occur at the interface. As is discussed below, binding of the charged form can be ruled out by considering the extremely high surface density of the probe at saturation and, according to the results presented here, the second possibility would be more likely. This is also consistent with the requirement that, in order to use ACMA as a $\Delta$pH-responding probe, only the neutral form of the amine must be freely permeable across the diffusable lipid barrier (this process depending on the proton concentration difference between the outer and inner osmotic compartments).

When the internal and external pH are equal, i.e. in the dark and in the absence of any proton pumping activity, a symmetrical distribution of the probe in the two aqueous compartments can be assumed ($C_o = C_i$). Moreover, given the small internal volume of the chromatophore membranes [in the range of 15 μl μ*M* $BChl^{-1}$, as determined from Tempone distribution in EPR experiments by Melandri et al. (1984)] compared with that of the external water phase, $C_i V_i$ in Eq. (2) can be neglected. As an approximation, the surface densities of the adsorbed molecules can also be considered to be symmetrical, provided that the adsorbing isotherm is assumed to be identical on both sides of the membrane. Under these conditions Eq. (2) simplifies to:

$$n^T_{(ACMA)} = C_o V_o + \sigma (S_i + S_o) . \quad (3)$$

The data shown in Table 1 can, therefore, be used for a quantitative evaluation of the adsorbing isotherm. This is shown in Fig. 3, (curve a) where the concentration of ACMA free in the aqueous solution is related to the number of nanomoles within the membrane phase ($\sigma S$). The relationship between these values is best fitted (least

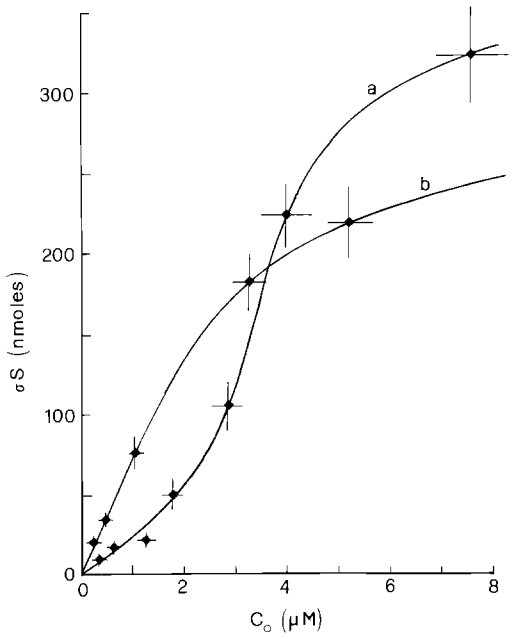


**Fig. 3.** Partitioning of ACMA between the aqueous phase and the membrane interface. Curve (a): adsorption isotherm with $K_A = 26.6\ \mu M$; $\sigma_{max} S = 513.4$ nmoles; $A = -1.08 \times 10^{-2}$ nmoles$^{-1}$. $\sigma S$ values (the number of ACMA nanomoles adsorbed to the total adsorbing membrane surface) are obtained from the overall mass balance at different ACMA concentrations [Eq. (3)] and from the nanomoles of the probe found free in the supernatants after pelletting chromatophores (Table 1, second row). Curve (b): desorption isotherm with $K_A = 6.2\ \mu M$; $\sigma_{max} S = 413$ nmoles; $A = -6.54 \times 10^{-3}$ nmoles$^{-1}$. In this case, the number of ACMA nanomoles recovered after solubilization of the pellets is plotted as a function of the probe concentration found free in the supernatant upon re-suspending and re-pelletting the first pellets (third and fourth rows in Table 1). The experimental conditions are detailed in the Materials and methods section. The values of pH, ionic strength and temperature of the assay medium are 8.5, 0.1 $M$ and 25 °C, respectively

squares analysis) when the following adsorbing isotherm is used:

$$C_{o,i} = K_A \cdot \frac{\sigma S}{\sigma_{max} S - \sigma S} \cdot \exp\left(\frac{\sigma S}{\sigma_{max} S - \sigma S} + A \cdot \sigma S\right), \quad (4)$$

where $C_{o,i}$ is the concentration of the amine free in the aqueous volumes, $V_o$ an $V_i$; $\sigma$ is the surface density of the amine; $S$ is the total adsorbing surface of the membrane (equal to the total sum of the internal and external surfaces) and $\sigma S$ is the nanomoles of probe bound to the membrane (experimentally evaluated).

The above equation is strictly related to the adsorption isotherm derived by Hill (1946) on the basis of statistical quantum-mechanics to describe multi-molecular adsorption of a two-dimensional van der Waals gas onto a non-ideal, non-localized monolayer, when lateral attraction within the monolayer becomes significant (see Appendix). This then allows an interpretation of the three parameters $K_A$, $\sigma_{max}$ and $A$ in terms of molecular parameters with a consequent evaluation of the interactions between ACMA molecules within the adsorbing surface (see Appendix).

The data shown in Table 1 can also be used to test whether desorption is symmetrical with respect to adsorption. With the same arguments used above, the concentrations of ACMA, determined after resuspending and re-pelletting the membranes (third row), are related to the nanomoles of the probe remaining in the membrane phase and measured after solubilization of the pellets (fourth row). The experimental data can still be fitted to the $S$-shaped isotherm described by Eq. (4). However, it is quite evident that the adsorption and desorption branches of the isotherm are not coincident over the whole range of concentrations tested (Fig. 3, curve b). The fitting parameters $K_A$, $\sigma_{max} S$ and $A$ are found to be different, as a consequence of the hysterisis loop observed. This may be interpreted as indicating that the interactions between adsorbate and adsorbent are different for the desorption and adsorption pathways (see Appendix).

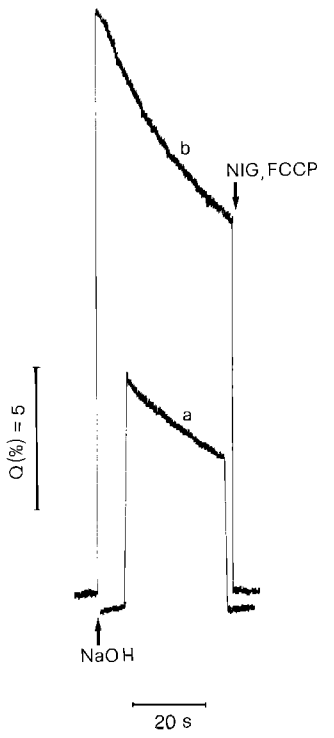


**Fig. 4.** Quenching of ACMA fluorescence induced by imposing artificial transmembrane $\Delta$pH's. Curve (a): $\Delta pH = 0.43 \pm 0.05$; curve (b): $\Delta pH = 0.68 \pm 0.05$. The initial pH value is $5.55 \pm 0.05$. Nigericin (NIG) or FCCP are added at a final concentration of 2 $\mu M$

*Calibration of the quenching of ACMA fluorescence in terms of ΔpH's of known extents*

When acid to base transitions are imposed on the assay medium containing known concentrations of ACMA and chromatophore membranes a quenching of the fluorescence of the probe is detected (Fig. 4). Its extent increases for increasing $\Delta$pH values and, in this way, a calibration of the quenching of fluorescence in terms of $\Delta$pH can be obtained. The experimental data points are shown in Fig. 5. This phenomenon, which is caused by a transient alkalinization of the external medium with respect to the internal aqueous compartment of the chromatophore membranes, fully decays in about 200 s, or more, depend-

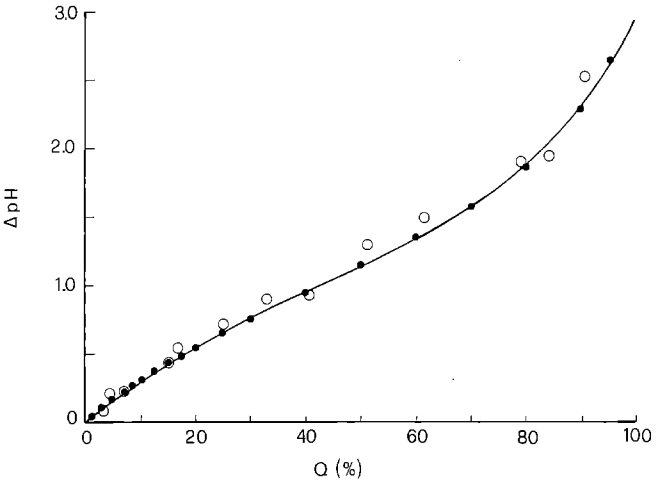


**Fig. 5.** Dependence of $\Delta$pH on the quenching of ACMA fluorescence. Comparison between the experimental (o) and theoretical (•) $\Delta$pH values as obtained from the empirical calibration and from the model, respectively. The data are shown as a function of the $Q$ values. Curve fitting is performed according to Eq. (7), with $A=6.2$; $B=175$; $C=-2.2\times10^{-2}$. The best fit for the theoretical values coincides with that of the experimental $\Delta$pH's

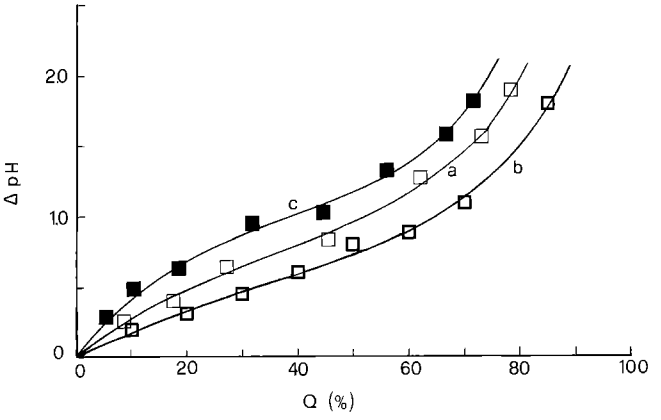


**Fig. 6.** Curves of calibration of the quenching of ACMA fluorescence in terms of $\Delta$pH under different experimental conditions. Curve fitting of the experimental data points (shown) is performed as in Fig. 5, with Eq. (7) using the $A$, $B$ and $C$ values determined from the fitting of the corresponding theoretical $\Delta$pH's. Curve (a): control experiment (BChl 30 $\mu M$) with $A=4.5$, $B=142$ and $C=-2.9\times10^{-2}$; curve (b): in the presence of a 2 fold BChl concentration (60 $\mu M$) as compared to curve (a), with $A=3$, $B=151$ and $C=-2.5\times10^{-2}$; curve (c): as curve (a), in the presence of 1.25 $M$ sucrose to increase the osmolarity of the assay medium with $A=6.6$, $B=168$ and $C=-2.5\times10^{-2}$. Under these conditions, the value of the inner volume is 15 fold decreased with respect to the control and is equal to 1 $\mu$l · $\mu$mol · BChl$^{-1}$

ing on the membrane passive permeability, which may change in different preparations. It is, however, accelerated about 200 fold when known effectors of the transmembrane $\Delta$pH and/or $\Delta\psi$ are added to the assay medium. The onset of the quenching is mono-exponential, as shown by kinetic analysis of traces obtained in rapid mixing experiments. The half time of the process is about 150 ms at 22 °C, and this value is not affected when divalent cations, such as $Mg^{+2}$ or $Ca^{+2}$, are added to the

**Table 2.** Half-time of the onset of the quenching of ACMA fluorescence induced by an artificial $\Delta$pH

| Additions | $t_{1/2}\pm\Delta t_{1/2}$ (ms) |
|---|---|
| – | 149±38 |
| +5 m$M$ $MgCl_2$ | 149±54 |
| +5 m$M$ $CaCl_2$ | 172±23 |

The half time ($t_{1/2}$) is obtained from kinetic analysis of the onset of the quenching of ACMA fluorescence as detected in experiments of rapid mixing. The onset is fitted by a mono-exponential function and the total quenching is 50–55%. The average value obtained from ten different experiments for each condition is shown. Temperature was 22 °C

assay medium (see Table 2). Moreover, the addition of divalent cations at a concentration of 5 m$M$ does not significantly affect also the extent of the quenching of fluorescence detected upon imposing each acid to base transition. In contrast, the $Q$ values can be modulated by changing the inner volume of the chromatophore membranes. This is achieved either by increasing the osmolarity of the assay medium, or by increasing the concentration of BChl. For each artificially induced $\Delta$pH, as compared to the control experiment, the extent of the quenching of fluorescence decreases in the former and increases in the latter case. These results are shown in Fig. 6, where a theoretical relation between $\Delta$pH and $Q$ is established. In these experiments, the probe-BChl molar ratio was 0.25. This value was chosen after finding that the extent of the quenching of fluorescence, at a transmembrane imposed $\Delta$pH, was independent of the probe-BChl molar ratio for values in the range 0.1 to 0.4. Under these conditions, the coupling properties of the chromatophore membranes (namely photophosphorylation and ATPase activity) were also unaffected.

### *Determination of the transmembrane $\Delta$pH as a function of the quenching of fluorescence and correction for the adsorption of the probe on the membrane interface*

The question that arises is whether it is possible to relate the experimental data observed to a model, according to which the transmembrane $\Delta$pH is determined by considering the probe-membrane interactions.

We can then use the model of Eq. (1), taking into consideration the contribution of the neutral molecule-monocation equilibrium (Rottenberg 1979) and provided that the internal volume is independently evaluated:

$$pH_i = -\mathrm{Log}\left[\frac{C_i}{C_o}(10^{-pH_o}+10^{-pK_a})-10^{-pK_a}\right], \qquad (5)$$

where $C_i$ and $C_o$ are the total internal and external concentrations of the amine, and $pH_o$, $pH_i$ and $pK_a$ are the external and internal pH and the $pK_a$ of the monocation-neutral molecule equilibrium, respectively.

The concentration ratio in Eq. (5) is that of the amine free in the aqueous internal and external compartments. In the case of a probe which interacts strongly with the

membrane, such as ACMA, (see previous section), the free concentrations in the inner and outer compartments can be calculated only by taking its adsorption into account.

This can be done by using Eq. (2), as determined above, provided that it is assumed that only the neutral form of the amine is freely permeable through the diffusion barrier. The free concentrations of the probe in the outer and inner bulk phases are related to the amount adsorbed at the corresponding membrane face by Eq. (4), in which the parameters $\sigma_{max} S$ and $A$, which include the surface value, are obtained from those determined in the absence of a $\Delta$pH by expressing the outer and inner surfaces as a fraction of the total surface. This relies on the assumption that the surface density of the probe at saturation is not affected by the presence of a $\Delta$pH. Following the steps of partitioning of the probe according to Eq. (2), the adsorption and desorption branches of the "binding" isotherm are associated with the outer and inner membrane faces, respectively.

The external concentration of ACMA ($C_o$) in equilibrium with the chromatophore membrane in the absence of any $\Delta$pH can be experimentally determined and is also known from Eq. (4). The concentration of the probe free in the aqueous external compartment which corresponds to a certain quenching of fluorescence, ($C'_o$), can then be calculated as:

$$C'_o = C_o - C_o \cdot Q \tag{6}$$

This equation depends on the idea that the only fluorescent form of the amine is that free in the aqueous external buffer (see above). From this, by considering the adsorption isotherm, and from the mass balance of Eq. (2), the nanomoles of probe to be found in the inner interface and aqueous phase can be calculated. Subsequently, by using the desorption isotherm, the internal free concentration of the probe is evaluated, assuming for $V_i$ the value of the inner volume calculated from EPR experiments (Melandri et a. 1984) and considering that the area of the internal desorbing surface is one third of that of the adsorbing one, as detailed in the Materials and methods section.

According to this model, when the concentrations of ACMA and BChl in the assay are respectively 5 and 21 $\mu M$, at $\Delta$pH and $Q$ equal to zero, only 25% of the probe is free in the aqueous phase after equilibrating with the membrane phase (see also Table 1). When $Q$ ranges from 1 to 95% of the initial level of fluorescence, in the presence of chromatophores, the amount of ACMA free in the solution (outer and inner volumes) decrease from 25 to 1% of the total amount, the remainder being adsorbed on the total adsorbing surface of the membrane. Concomitantly, the ratio between the amount free in the inner osmotic space to that in the total aqueous compartment ranges from $3 \times 10^{-4}$ to $7.9 \times 10^{-2}$, i.e. the amount of ACMA free in the inner volume, at increasing $Q$, changes from $9 \times 10^{-4}$ to $10^{-1}$% of the total amount of the probe added to the assay medium. $C_i$, in turn, ranges from the $C_o$ value of 1.27 to 16.26 $\mu M$, at a $Q$ value of 95%.

Solutions to Eq. (4) are obtained only numerically so that no simple analytical function relating $\Delta$pH and $Q$ can be derived. However, with the procedure detailed above and from Eq. (5) it is possible to calculate, for each quenching of fluorescence observed, a corresponding $\Delta$pH. The relation between $\Delta$pH and $Q$ can then be obtained from the best fit to the calculated data points and is described by the following equation:

$$\Delta\text{pH} = A \cdot \frac{Q}{B-Q} \exp\left(\frac{Q}{B-Q} + C \cdot Q\right), \tag{7}$$

where $A$, $B$ and $C$ are three empirical fitting parameters.

Figure 5 shows the fit of the theoretical curve to the experimental data points obtained in a calibration experiment for fluorescence quenching, when both the $\Delta$pH and $Q$ values were independently measured. It is evident that the model can predict the observed dependence of $\Delta$pH on the quenching of ACMA fluorescence within experimental error.

As described above, the experiments of calibration are also performed in the presence of sucrose, to decrease the inner osmotic volume, and with chromatophores corresponding to a higher BChl concentration (see the previous section). The results are shown in Fig. 6. The fitting of curves a and b, as compared to the curve shown in Fig. 5, is performed after a re-evaluation of the parameters of the adsorbing-desorbing isotherm, due to the increase of the total membrane surface. These values are consistent with what can be predicted from geometrical considerations, assuming a spherical shell model for the vesicle and a constant total surface area per nanomole of BChl (see Appendix). A consequent normalization of the value of the inner volume to the BChl concentration is also necessary. When the osmolarity of the assay medium is about fifteen fold higher than in the control (Fig. 6, curve c), the fit is obtained by assuming a value of the inner volume fifteen fold lower than that of the control experiments. The decrease of the value of the osmotic volume is consistent with what is observed experimentally on measuring this parameter at the same osmolarity in EPR experiments (Melandri et al. 1984).

## Discussion

The results presented in this work indicate that, in spite of its large adsorption on the membrane phase, ACMA can still be used as a reliable tool for the measurement of transmembrane $\Delta$pH in a range of values not detectable with other probes. This conclusion is based on the fact that it is possible to predict the dependence of $\Delta$pH on the quenching of fluorescence by using a model in which adsorption of the probe on the membrane is taken into account to evaluate its redistribution between the outer and inner osmotic volumes following the application of a $\Delta$pH.

By applying this correction, a nonlinear dependence between $Q$ and $\Delta$pH is established. The fitting parameters may then be used to calculate a $\Delta$pH value from a measured value of $Q$. If one accepts that the artificially imposed pH difference simulates the formation of a transmembrane proton concentration difference, the empirical calibration curve that we found [Eq. (7)] can be used to

evaluate, under the same experimental conditions and with the same membrane system, a $\Delta$pH value corresponding to a certain quenching of fluorescence, for $Q$ values from 3 to about 80%. At higher $Q$ values Eq. (7) predicts unrealistically high $\Delta$pH values. This procedure can be extended to any membrane system, provided that adsorption of the probe is similarly characterized. Probe-membrane interactions may be measured for a wide range of ACMA concentrations, to quantitate the overall pattern of binding [Eq. (4)], and used for correcting for adsorption. Nevertheless, when the transmembrane $\Delta$pH is detected the probe is used only in a limited range of concentrations (routinely corresponding to a probe-BChl molar ratio ranging from about 0.1 to 0.4) in order not to affect the coupling properties of the membranes. Under these conditions, the total load of the probe in the membrane, even at the highest $Q$ values, is well below its surface density at saturation (see Appendix), which would probably correspond to a highly modified membrane organization. In the model described here the relevant parameters are the adsorbing-desorbing constant ($K_A$), the saturation surface density of the probe ($\sigma_{max}$), and the total adsorption-desorption surface area ($S$). When correcting for probe-membrane interactions using the binding isotherm [Eq. (4)] together with the mass balance equation [Eq. (2)], the $V_i$ value may change by a factor of five (at constant adsorbing area) on changing $\Delta$pH by only 0.05 units. This would then include possible over- or under-estimations of the $V_i$ value as determined with EPR (Wille 1988).

Our model is based on the following basic assumptions: a) the only fluorescent form of the amine is that free in the aqueous environment; b) the free amine behaves ideally; only its neutral form diffuses freely through the membrane phase and Eq. (5) holds; c) the adsorption of the probe on the membrane can be described by Eq. (4).

Regarding point a), the assumption is based on the evidence presented in this study. In the presence of both de-energized and energized chromatophores neither the absorbance, nor the excitation and emission spectra of the probe are distorted or altered. The splitting observed in the emission spectrum of ACMA upon addition of chromatophores to the assay medium is compensated for by correcting for inner filter effects. It is, however, noticeable that both the excitation and emission spectra undergo a marked decrease in intensity, which occurs predominantly upon addition of the membranes in the dark. The effect can be further increased in the presence of a light induced $\Delta$pH. These observations can be accounted for by considering that hypochromic effects may occur within the membrane domain owing to stacking and accumulation of the chromophores in this environment of low dielectric constant. Consistent with this, it is reported that the excitation and emission spectra of the dye are progressively shifted to shorter wavelengths when it is dissolved in apolar solvents (Marty and Viallet 1982) and that the relative quantum yield of fluorescence is also greatly decreased (our data not shown). Huang et al. (1982) used fluorescence polarization to study the interaction of 9-amino-3-chloro-7-methoxyacridine (a parent molecule of ACMA) with sub-mitochondrial membranes and showed that the probe behaves as a freely rotating fluorescence emitter only when it is free in the aqueous compartment.

According to our results any dye molecule associated with the membrane phase would be non-fluorescent in the 400–650 nm region. No evidence for dimerization of the probe could be detected in solution [compare also Marty and Viallet (1987)] and in the presence of de-energized or energized membranes, in contrast to what has been reported by Torres-Pereira et al. (1984) when working with illuminated chloroplasts. Recently it has been shown, using 9-AA in phosphatydilserine vesicles (Grzesiek and Dencher 1988; Grzesiek et al. 1989), that is is necessary to have a negatively charged surface in order to promote excimer formation at the membrane upon $\Delta$pH formation. The interpretation of the discrepancy between our results and those of other workers would then be that the surface of energized chromatophores is less negatively charged than that of chloroplast, probably due to the higher ionic strength of our assay medium. In chromatophores, however, according to the adsorption isotherm [Eq. (4)], most of the dye is already associated with the membrane in the dark. Any further binding, promoted by $\Delta$pH formation, is negligible in terms of mass displacement from the outer to the inner side of the membrane. It is therefore unlikely that dimerization, if any, would occur only in the presence of a $\Delta$pH. Moreover, using the same argument, the contribution to the fluorescence from the molecules free in the inner aqueous volume can be neglected, even at the highest $Q$ values. Regarding point b), it is the general assumption underlying the use of amines to detect transmembrane pH (Rottenberg et al. 1972; Schuldiner et al. 1972) and results mainly from studies on the mechanism of amine transport in chloroplasts. In the case of fluorescent amines, it has been shown that the partition coefficient of the 9-aminoacridine monocation is zero (in contrast to its neutral form) in a variety of hydrophobic solvents (Pick 1976). Our data confirm the validity of this assumption since we find that adsorption of ACMA on the membrane does not depend on the concentration of the monocation relative to that of the neutral form. This suggests that the protonation-deprotonation equilibria occur at the solution-membrane interface before partitioning into the hydrocarbon. At the ionic strength used in our experiments ($I = 0.1\,M$), stacking appears to be largely non-electrostatic in nature as it is by increasing the ionic strength to $0.25\,M$. ACMA adsorption on the membrane is mainly driven by highly favorable hydrophobic interactions and can be fully reversed only upon solubilization of the membrane.

A further argument supporting this point is the extremely high surface density that we calculate for saturation (see Appendix). This corresponds to one ACMA per one to four lipid molecules depending on whether the total adsorbing surface is or is not limited to the lipid surface. This figure is at least one order of magnitude higher than that found for most hydrophobic cations and anions tested, the hydrophobic surface and ionic radius of which should be similar to that of ACMA. It is generally accepted (Flewelling and Hubbel 1986a, b) that binding saturation of hydrophobic ions, which interact in the

membrane boundary regions with a dipole potential a few hundred millivolts positive inside, is reached when the electrostatic interaction energy in the low dielectric constant medium is compensated for by the average thermal energy. If ACMA were adsorbed as a monocation in the boundary regions, its binding would also saturate at a lower surface density.

The data obtained when partitioning of ACMA is determined (point c)) are interpreted by neglecting any possible overestimation of binding due to dark Donnan potentials, which under our experimental conditions can be estimated to be less than 0.1 unit (Haraux and De Kouckovsky 1980). As the results shown in Table 1 indicate, binding of ACMA to the chromatophore membranes is concentration-dependent (as well as, within the experimental limits considered, pH and ionic strength-independent). Thus, our interpretation of the probe-membrane interactions is described in terms of adsorption and not of partitioning between the aqueous and the membrane phases, as previously, suggested for 9AA in chloroplasts (de Kouchkovsky et al. 1984). This argument also considers the low solubility of ACMA in organic solvents (our results, not shown). Electrostatic effects are not included in our model because they are apparently negligible for the ionic strengths considered. Other authors, when investigating the interactions of 9AA with chloroplast membranes, concluded that for the range of ionic strengths used in our experiments, screening of the charges at the membrane surface was almost saturated and the probe-membrane interaction was negligible (Searle and Barber 1978; Haraux and de Kouchkovsky 1980; Hope and Matthews 1985). Based on the findings that monovalent and/or divalent cations were able to displace much of the amine bound to the membrane, and that probe-membrane interactions were pH-dependent at low ionic strength values, it was concluded that binding was mainly electrostatic and due to the cationic form of the molecule. Consistently, adsorption was described and modelled as occurring at specific, negatively charged, binding sites located at the membrane surface (Hope and Matthews 1985; Vu Van et al. 1987). In our membrane system, although it is characterized by a surface charge density similar to that of chloroplast under de-energized conditions (about 2 $\mu C\ cm^{-2}$, our work in preparation), the adsorption of ACMA is also extensive at high ionic strengths. Furthermore, it not affected when the monocation concentration is almost doubled with respect to that of the neutral form by changing the pH. According to these results, any model relying on specific adsorption at saturable binding sites, which can be screened when the ionic strength of the bulk solution is increased up to 0.1 $M$ or higher, is not suited to describe our experimental data. However, we cannot, in principle, exclude the possibility that electrostatic effects play a major role in binding phenomena at ionic strength values lower than those used here.

The results are then fitted to an $S$-shaped isotherm, which is generally indicative of strong intermolecular interactions within the adsorbed layer. This is likely to occur when the major axis of the adsorbed molecule is perpendicular to the surface and the adsorbate is monofunctional (Kipling 1965; Aveyard and Haydon 1973). The use of the Hill isotherm to describe adsorption is based purely on the coincidence between this equation and the best fit of our experimental data. This is not a sufficient test of the theory (a detailed analysis of the binding dependence on the temperature would be also necessary), but it does allow one to quantitate ACMA interactions within the adsorbed layer, evaluating molecular parameters such as the co-area and the co-pressure. Noticeably, adsorption of ACMA is hysteretic, as in the case of porous adsorbents (Aveyard and Haydon 1973; Marino Bettolo Marconi and Van Swol 1989). At the present time this analogy is totally empirical and the behaviour observed may be a consequence of the extremely high hydrophobicity of the molecule. In our model, hysteresis is considered by combining the adsorption and desorption branches of the Hill isotherm to describe binding equilibria between the outer and inner aqueous compartments and the membrane. In order to simulate the empirical calibration curve we need, in addition, to assume that the inner desorbing surface is about one third of the external adsorbing one. This ratio is higher than that expected when considering a spherical shell model for the choromatophore membrane (1 : 2); it is consistent with the asymmetric distribution of lipid molecules in these membranes [the inner surface density of membrane proteins is about two-fold higher than the outer (Casadio et al. 1984)], confirming that binding of ACMA occurs via adsorption restricted to the lipid phase.

## Appendix

On the basis of statistical mechanics and thermodynamics, by assuming a mobile first layer on the adsorbing surface and by considering equilibrium between the chemical potentials of the adsorbed and gas phases, it was possible to derive a multimolecular adsorption isotherm for a gas obeying the van der Waal's equation in two dimensions [see Hill (1946)]. At low pressures, the adsorption isotherm simplifies to:

$$x = \frac{1}{C} \cdot \frac{\vartheta}{1-\vartheta} \cdot \exp\left(\frac{\vartheta}{1-\vartheta} - \alpha\vartheta\right) \tag{8}$$

where $x$ = molar fraction of the adsorbing gas;

$$C = \frac{b' j j_N}{j_L} \cdot \frac{2\pi m k T}{h^2} \cdot \exp\left[(\varepsilon_1 - \varepsilon_L)/k T\right]$$

in which $j$ is the internal partition function; $j_N$ the partition function for vibration normal to the surface; $-\varepsilon_1$ is the potential energy of a molecule in the first layer due to interaction between the molecule and the surface; $j_L$ and $-\varepsilon_L$ the partition function and the potential energy of molecules in higher layers which are assumed to be liquid like; $m$ the mass of the molecule; $k$ and $h$ are the Boltzmann and Planck constants, respectively, and $T$ the absolute temperature.

$\vartheta = N\, b'/S$

in which $N$ is the number of molecules adsorbed in the area $S$ and $b'$ is the so called co-area in the van der Waal's equation.

$$\alpha = 2a'/b'kT$$

in which $a'$ is the other constant of the two-dimensional van der Waal's equation or co-pressure.

The isotherm derived by Hill is coincident with Eq. (3), by considering, instead of the molar fraction of the gas, the concentration of ACMA free in the aqueous solution; by making $K_A$ proportional to $1/C$ and $N/S$ equal to $\sigma$, the surface density of the adsorbate. It can be easily verified that, under these conditions, in Eq. (3):

$$\sigma_{max} = 1/b' ; \quad A = 2a'/kTS .$$

Provided that the total adsorbing surface is independently evaluated it is possible to estimate $b'$ and $a'$ from the theoretical fitting of the adsorption and desorption data. The outer surface of a chromatophore is equal to about $8 \times 10^{-15}$ m$^2$. This can be calculated by assuming, for simplicity, a spherical shell model for these vesicles and using the average diameter distribution measured by analyzing electron micrographs of freeze-etched populations (Casadio et al. 1988). By considering that a single vesicle contains about $3 \times 10^3$ molecules of BChl (Saphon et al. 1975), and has a membrane thickness of 5 nm, a total adsorbing surface of $3.2 \times 10^{-3}$ m$^2$ per BChl nanomole can be estimated. From this value, and from the values of the fitting parameters of the adsorption isotherm, a saturating surface concentration of about 0.6 molecule of ACMA per nm$^2$, which corresponds to a $b'$ value of 1.7 nm$^2$ molecule$^{-1}$, is computed; $a'$, in turn, is $2 \times 10^{-20}$ J nm$^2$ molecule$^{-1}$. These constants are 2.5 nm$^2$ molecule$^{-1}$, and $1 \times 10^{-20}$ J nm$^2$ molecule$^{-1}$, respectively, when evaluated from the fitting parameters of the desorption branch of the isotherm. In chromatophores, given the phospholipid to protein weight ratio (Casadio et al. 1984, 1988) and assuming an average surface area of 20 nm$^2$ for a membrane protein, it can be calculated, as a lower limit, that half of the total adsorbing surface is occupied by lipid molecules. If so, the saturating surface concentration of ACMA, would be further increased by a factor of two, both for adsorption and desorption, corresponding to about one ACMA per one and two lipid molecules, respectively.

## References


Albert A (1966) The acridines – Their preparation, physical, chemical and biological properties and uses. Edward Arnold, London

Aveyard R, Haydon DA (1973) An introduction to the principles of surface chemistry. Cambridge University Press, London

Azzone GF, Pietrobon D, Zoratti M (1984) Determination of the proton electrochemical gradient across biological membranes. Curr Top Bioenerg 13:2–77

Baccarini Melandri A, Melandri BA (1971) Partial resolution of the photophosphorylation system of *Rhodopseudomonas capsulata*. Methods Enzymol 123:556–561

Baccarini Melandri A, Casadio R, Melandri BA (1981) Electron transport, proton translocation and ATP synthesis in bacterial chromatophores. Curr Top Bioenerg 12:197–258

Bevington PR (1969) Data reduction and error analysis for the physical sciences. McGraw-Hill, New York

Brandt L, Witholt B (1967) Fluorescence measurements. Methods Enzymol 9:776–856

Capomacchia AC, Schulman SG (1975) Electronic absorption and fluorescence spectrophotometry of quinacrine. Anal Chim Acta 77:79–85

Casadio R (1988) The oligomycin-sensitive Ca-ATPase of chromatophores from photosynthetic bacteria is not coupled to $\Delta\bar{\mu}_{H^+}$ generation. In: Ion pumps: structure, function and regulation. AR Liss, New York pp 201–206

Casadio R, Melandri BA (1977) The behaviour of 9-aminoacridine as an indicator of transmembrane pH difference in liposomes of natural bacterial phospholipids. J Bioenerg Biomem 9:17–29

Casadio R, Melandri BA (1984) On the regulation of the ATPase activity in chromatophores of *Rhodopseudomonas sphaeroides*. In: Papa S, Altendorf K, Ernester L, Packer L (eds) $H^+$-ATPase (ATPsynthase): structure, function, biogenesis. The $F_0F_1$ complex of coupling membranes. ICSU Press, Adriatica Editrice, Bari pp 411–420

Casadio R, Melandri BA (1985) Calibration of the response of 9-aminoacridine fluorescence to transmembrane pH differences in bacterial chromatophores. Arch Biochem Biophys 238:219–228

Casadio R, Venturoli G, Di Gioia A, Castellani P, Leonardi L, Melandri BA (1984) Phospholipid-enriched bacterial chromatophores. A system suited to investigate the ubiquinone-mediated interactions of protein complexes in photosynthetic oxidoreduction processes. J Biol Chem 259:9149–9157

Casadio R, Venturoli G, Melandri BA (1988) Evaluation of the electrical capacitance in biological membranes at different phospholipid to protein ratios. A study in photosynthetic bacterial chromatophores based on electrochromic effects. Eur Biophys J 16:243–253

Clayton RK (1963) Towards the isolation of a photochemical reaction center in *Rhodopseudomonas sphaeroides*. Biochim Biophys Acta 75:312–323

Deamer DW, Prince RC, Crofts AR (1972) The response of fluorescent amines to pH gradients across liposome membranes. Biochim Biophys Acta 274:323–335

Dufour JP, Goffeau A, Tsong TY (1982) Active proton uptake in lipid vesicles reconstituted with the purified yeast plasma membrane ATPase. Fluorescence quenching of 9-amino 6-chloro 2-methoxyacridine. J Biol Chem 257:9365–9371

Fiolet JW, Bakker EP, Van Dam K (1974) The fluorescence properties of acridines in the presence of chloroplasts or lyposomes. On the quantitative relationship between the fluorescence quenching and the transmembrane proton gradient. Biochim Biophys Acta 368:432–445

Flewelling RF, Hubbel WJ (1986) Hydrophobic ion interactions with membranes thermodynamic analysis of tetraphenylphosphonium binding to vesicles. Biophys J 49:531–540

Flewelling RF, Hubbel WL (1986) The membrane dipole potential in a total membrane potential model. Applications to hydrophobic ion interactions with membranes. Biophys J 49:541–552

Friedl P, Friedl C, Schairer HU (1979) The ATP synthetase of Escherichia coli K12: purification of the enzyme and reconstitution of energy transducing activities. Eur J Biochem 100:175–180

Gangola P, Joshi NB, Pant DD (1981) Excimer emission in 9-aminoacridine hydrochloride. Chem Phys Lett 80:418–421

Grzesiek S, Dencher NA (1988) The $\Delta$pH-probe 9-aminoacridine: response time, binding behaviour and dimerization at the membrane. Biochim Biophys Acta 938:411–424

Grzesiek S, Otto H, Dencher NA (1989) $\Delta$pH-induced fluorescence quenching of 9-aminoacridine in lipid vesicles is due to excimer formation at the membrane. Biophys J 55:1101–1109

Haraux F, de Kouchkovsky Y (1980) Measurements of chloroplast internal protons with 9-aminoacridine. Probe binding, dark proton gradient and salt effects. Biochim Biophys Acta 592:153–168

Hill TL (1946) Statistical mechanics of multimolecular adsorption. Localized and mobile adsorption and desorption. J Chem Phys 14:441–453

Hope AB, Matthews DB (1985) Adsorption of amines to thylakoid surfaces and estimation of $\Delta$pH. Aust J Plant Physiol 12:9–19

Huang CS, Kopacz SJ, Lee CP (1983) Mechanistic differences in the energy linked fluorescence decreases of 9-aminoacridine dyes associated with bovine heart submitochondrial membranes. Biochim Biophys Acta 722:107–115

Kamlet MJ, Abbond JL, Taft RW (1977) The solvatochromic comparison method 6. The $\pi^*$ scale of solvent polarities. J Am Chem Soc 99:6027–6038

Kipling JJ (1965) Adsorption from solutions of non-electrolytes. Academic Press, London New York

Kouchkovsky Y de, Haraux F, Sigalat C (1984) A microchemiosmotic interpretation of energy-dependent processes in biomembranes based on the photosynthetic behaviour of thylakoids. Bioelectrochem Bioenerg 13:143–162

Kraayenhof R, Fiolet JWT (1974) On the interaction of 9-amino substituted acridine probes with energy conserving membranes. In: Ernester L, Estabrook RW, Slater EC (eds) Dynamics of energy transducing membranes. Elsevier, Amsterdam, pp 355–363

Lowry OH, Rosebrough NJ, Farr AL, Randall RJ (1951) Protein measurements with the Folin phenol reagent. J Biol Chem 193:265–275

Malpartida F, Serrano R (1981) Proton translocation catalyzed by the purified yeast plasma membrane ATPase reconstituted in liposomes. FEBS Lett 131:351–355

Marini Bettolo Marconi H, Van Swol F (1989) A model of hysteresis in narrow pores. Europhys Lett 8:531–535

Marty A, Viallet P (1982) Essais d'interprétation des déplacements des spectres électroniques de diverses amino-9 acridines en solution par leurs interactions avec des solvants aprotiques. J Photochem 20:213–227

Marty A, Viallet P (1985) Application de la fluorimétrie de phase a l'étude des interactions soluté-solvant de quatre amino-9 acridines substitutées. J Photochem 28:71–85

Marty A, Bourdeaux M, Dell'Amico M, Viallet P (1986) 9-amino-2-methoxy-6-chloroacridinemonocation fluorescence analysis by phase-modulation fluorometry. Eur Biophys J 13:251–257

Melandri BA, Mehlhorn RJ, Packer L (1984) Light-induced proton gradients and internal volumes in chromatophores of *Rhodopseudomonas sphaeroides*. Arch Biochem Biophys 235:97–105

Pick U (1976) The pH gradient across chloroplast thylakoid membranes and its significance for photophosphorylation. PhD Dissertation, Weizmann Institute of Science, Rehovot, Israel

Rydstrom J (1979) Energy-linked nicotinamide nucleotide transhydrogenase properties of proton translocating and ATP-driven transhydrogenase reconstituted from synthetic phospholipids and purified transhydrogenase from beef heart mitochondria. J Biol Chem 254:8611–8619

Rottenberg H (1979) The measurement of membrane potential and $\Delta$pH in cells, organelles and vesicles. Methods Enzymol 45:547–569

Rottenberg H, Grunwald T, Avron M (1972) Determination of $\Delta$pH in chloroplasts. 1 Distribution of [$^{14}$C] Methylamine. Eur J Biochem 1972:54–63

Saphon S, Jackson JB, Lerbs W, Witt HT (1975) The functional unit of electrical events and phosphorylation in chromatophores from *Rhodopseudomonas sphaeroides*. Biochim Biophys Acta 408:58–66

Schuldiner S, Rottenberg H, Avron M (1972) Determination of $\Delta$pH in chloroplasts. 2 Fluorescent amines as a probe for the determination of $\Delta$pH in chloroplasts. Eur J Biochem 1972:64–70

Searle GFW, Barber J (1978) The involvement of the electrical double layer in the quenching of 9-aminoacridine fluorescence by negatively charged surface. Biochim Biophys Acta 502:309–320

Strotmann H, Lohse D (1988) Determination of the $H^+$ transport-coupled reversible chloroplast ATPase reaction by equilibrium studies. FEBS Lett 229:308–312

Torres-Pereira JMG, Wong Fong Sang HW, Theuvenet APR, Kraayenhof R (1984) Electric surface charge dynamics of chloroplasts thylakoid membranes. Temperature dependence of electrokinetic potential and aminoacridine interaction. Biochim Biophys Acta 767:295–303

Vu Van T, Heinze T, Buchholz J, Rumberg B (1987) Quantitative relationship between 9-aminoacridine fluorescence quenching and internal pH in broken chloroplasts. In: Biggins J (ed) Progress in photosynthesis researches vol III. Nijhoff, Dordrecht, pp 189–192

Wille B (1988) Thylakoid volume, proton translocation and buffering capacity as measured with spin-label techniques. Biochim Biophys Acta 936:513–530

William H (1986) Numerical recipes. Cambridge University Press, Cambridge